An investigation on the mechanics of nanometric cutting and the development of its test-bed

International Journal of Production Research, Vol.41 No.7, 2003, pp.1149-1165

X. Luo, K. Cheng*, X. Guo and R. Holt

School of Engineering, Leeds Metropolitan University

Calverley Street, Leeds LS1 3HE, UK (E-mail: k.cheng@lmu.ac.uk)

Abstract

The mechanics of machining at a very small depth of cut (100 nm or less) is not well understood. The chip formation physics, cutting forces generation, resulting temperatures and the size effects significantly affect the efficiency of the process and the surface quality of the workpiece. In this paper the cutting mechanics at nanometric scale is investigated in comparison with the conventional cutting principles. Molecular Dynamics (MD) is used to model and simulate the nanometric cutting processes. The models and simulated results are evaluated and validated by the cutting trials on an atomic force microscope (AFM). Furthermore, the conceptual design of a bench type ultraprecision machine tools is presented and the machine aims to be a facility for nanometric cutting of 3D MEMS devices. The paper concludes with a discussion on the potential and applications of nanometric cutting techniques/equipment for the predictabilty, producibility and productivity in manufacturing at the nanoscale.

Key words: Nanometric cutting, MD simulation, atomic force microscope, ultraprecision machining, tool wear

*Correspondence to: Professor Kai Cheng, School of Engineering, Leeds Metropolitan University, Calverley Street, Leeds LS1 3HE, UK (E-mail: k.cheng@lmu.ac.uk)

Nomenclature

A Shear plane area, mm^2

a The elastic modulus, 1/m

B_i The bulk modulus, $1/m^3$

b Width of cut, mm

D The cohesion energy, J

d_c Depth of cut, mm

E_i The potential of the i-th atom, J

F A functional of cutting force

F_c The cutting force, N

$F(r_{ij})$ The interatomic force between atom i and atom j, N

F_s Shearing force, N

F_{ti} The force acting on the i-th cutting tool atom, N

F_{wi} The force acting on the i-th workpiece atom, N

F_{twi} The force acting on the i-th cutting tool atom from workpiece atoms, N

F_{tti} The force acting on the i-th cutting tool atom from other cutting tool atoms, N

F_{wti} The force acting on the i-th workpiece atom from cutting tool atoms, N

F_{wwi} The force acting on the i-th workpiece atom from other workpiece atoms, N

F_{wi} The force acting on the i-th workpiece atom, N

f_{0ij} Interatomic force in undeformed crystal, N

f_{ij} Interatomic force in deformed crystal, N

*Correspondence to: Professor Kai Cheng, School of Engineering, Leeds Metropolitan University, Calverley Street, Leeds LS1 3HE, UK (E-mail: k.cheng@lmu.ac.uk)

H Hamiltonian function

h Integral steps, s

h_c Hysteretic damping constant, Ns/m

m_{wi} The mass of workpiece atom

m_{ti} The mass of cutting tool atom

N The number of atoms

N_w The number of workpiece atoms

N_t The number of cutting tool atoms

q_i The position vector of the i-th atom, 10^{-9}m

P_s Shearing power, W

P_u Friction power, W

p_i The momentum of the i-th atom, Nm/s

r_{wi} The displacement vector of the i-th workpiece atom, 10^{-9}m

r_{ti} The displacement vector of the i-th cutting tool atom, 10^{-9}m

r_{ij} The distance between the atoms i and j, 10^{-9}m

r_i^n The displacement vector of the i-th atom at n integral step, 10^{-9}m

r_i^{n+1} The displacement vector of the i-th atom at n+1 integral step, 10^{-9}m

r_0 The atomic distance at equilibrium, 10^{-9}m

T Temperature, K

U Potential functional

u Morse potential energy, J

V_c Chip velocity, m/s

V_s Shearing velocity, m/s

v_i^n The velocity vector of the i-th atom at n integral step, m/s

v_i^{n+1} The velocity vector of the i-th atom at n+1 integral step, m/s

α_r Rake angle, deg

β_a Shear angle, deg

β_{c1} Nonlinear constant coefficient of stiffness function, 1/m

β_{c2} Nonlinear constant coefficient of stiffness function, $1/m^2$

ϕ_c Friction angle, deg

λ_a Interatomic stiffness, N/m

λ_s Slope of stiffness function at origin, N/m

σ The first principle stress, MPa

τ Cauchy stress, MPa

τ_s Shear stress, MPa

ω Chatter frequency, Hz

1 Introduction

Nanoscience and technology have been growing rapidly over recent years and, to some extent, are increasingly demanding manufacturing engineers to provide enabling techniques and equipment for fabrication of nanostructured materials, components, devices and systems and to lead to breakthroughs in manufacturability of new industrial products [1][2].

However, the physics of machining at nanometric scale, e.g. less than 100 nm, is not well understood. The chip formation mechanics, cutting forces generated, resulting temperatures and the size effects in the domain of nanometric cutting significantly affect the efficiency of the process and the surface quality of the workpiece. Furthermore, although traditional manufacturing techniques have been miniaturized for fabrication of microstructures as in semiconductors and microelectronics, the techniques are very difficult to cope with manufacturing the components with complex 3D features such as those on some optical and mechanical components (microlenses, micromoulds, laser targets). Therefore, it is much needed to carry out the fundamental research on nanometric machining and thus to address the underlying necessities for predictabilty, producibility and productivity in manufacturing at the nanoscale.

In this paper the authors present the preliminary results of the nanometric cutting research being undertaken at Leeds Metropolitan University. The research aims at:

- advancing the understanding of the ultraprecision machining process in general and the mechanics of nanometric cutting by MD simulations.
- integrating the machining process modelling, mathematical transforms including wavelet, chaos and fractal, and surface characterization for digital construction and functional control of precision engineering surfaces [3].
- developing the test-bed for nanometric cutting of a variety of engineering materials prescribed by the industry.

2 The mechanics of nanometric cutting

2.1 Nanometric cutting compared with conventional cutting

The research in nanometric machining requires new fundamental understanding of the phenomena defining the relationship between the materials and the processes. Because in nanometric cutting the depth of cut is down to 100 nm or less, the workpiece material cannot be regarded as a homogeneous media as that in conventional cutting since the presence of microstructure in the workpiece material is very distinct. Generally, the range of point defects, dislocations and crystal grain voids are 1-100 nm, 0.1 μm-10 μm and more than 10 μm respectively. Therefore, in nanometric cutting the formation of the chip intends to initiate from the point defects or dislocations in a crystal due to the small depth of cut. Furthermore, the deformation process of the workpiece surface/subsurface under the action of a cutting tool is different because the material property is variant with the crystal orientation and dislocation structure. Nanometric cutting in principle is thus quite different from that in conventional cutting. Table 1 summarises the comparison of nanometric cutting and conventional machining in all major aspects of cutting mechanics.

Table.1 The comparison of nanometric cutting with conventional cutting mechanics

		Nanometric cutting	**Conventional cutting** [4-6]
Fundamental Cutting principles		Discrete molecular mechanics/micromechanics [7-13]	Continuum elastic/plastic /fracture mechanics
Workpiece material		Heterogeneous [7-13] (presence of microstructure)	Homogeneous (ideal element)
Cutting physics		Atomic cluster or microelement model [7-13] $\dot{q}_i = \frac{\partial H}{\partial p_i}$ i=1, 2, … N $p_i = -\frac{\partial H}{\partial q_i}$	Shear plane model (continuous points in material)
		First principle stress [13] $\sigma = \frac{1}{S}\sum_{i=1}^{N_A}\sum_{j=1}^{N_B} f_{ij} - \frac{1}{S}\sum_{i=1}^{N_A}\sum_{j=1}^{N_B} f_{0ij}$ (crystal deformation included)	Cauchy stress principle $\tau_S = \frac{F_S}{A}$ (constant)
Cutting force and energy	Energy consideration	Interatomic potential functional [7-13] $U(r^N) = \sum_i \sum_{<i} u(r_{ij})$	Shear/friction power $P_s = F_s \cdot V_s$ $P_u = F_u \cdot V_c$
	Specific energy	High [8]	Low
	Cutting force	Interatomic forces [7-13] $F_I = \sum_{j\neq i}^{N} F_{ij} = \sum_{j\neq i}^{N} -\frac{du(r_{ij})}{dr_{ij}}$	Plastic deformation/friction $F_c = F(b, d_c, \tau_s, \beta_a, \phi_c, \alpha_r)$
Chip formation	Chip initiation	Inner crystal deformation [7] [8] (point defects or dislocation)	Inter crystal deformation (grain boundary void)
	Deformation and stress	Discontinuous	Continuous
Cutting tool	Cutting edge radius	Significant [7][8][12]	Ignored
	Tool wear	Clearance face and Cutting edge [14]	Rake face
Surface generation		Elastic recovery [7] [8]	Transfer of tool profile

The comparison in the table is by no means comprehensive, but rather provides a starting point for further study on the mechanics of nanometric cutting.

2.2 Characterization of nanometric cutting

Because nanometric cutting mainly occurs inside a crystal grain or may pass the grain boundary to the other crystal grain (in polycrystal), the cutting energy needs to break the atomic bond and overcome the resistance of the grain boundary. Conventionally, the cutting energy is shown in the form of interatomic forces between the cutting tool and workpiece material molecules. It is under the action of these interatomic forces the dislocation in the crystal grain initiates and with the movement of the dislocation, the chip is removed and the machined surface is generated. Therefore, the molecular mechanics and micromechanics play the fundamental role in studying the mechanics of nanometric machining. The mechanics of nanometric cutting is thus characterized with the following features:

- the machining unit in nanometric cutting is the atomic cluster, and the workpiece material is a discrete system.
- the cutting forces result from the interatomic forces between the molecules of the cutting tool and workpiece.
- the initiation of the chip formation commences at the point defects or dislocation in a crystal, and it needs much more energy to break the atomic bond, and the specific cutting energy is thus very high.
- deformation and strain within the workpiece material under the action of the cutting tool is discontinuous. In the cutting process, the deformation includes the internal deformation and interfacial deformation resulted from the interatomic forces or interaction forces between the crystal grains.

- the coefficient of friction between the cutting tool and workpiece materials is sensitive to the crystallographic orientation of cutting tool crystal. The crystalline orientation of the workpiece material has effect on the cutting force and the material shear strength.
- there is a "microstructure functional" which illustrates the relationship between the microstructure of the materials and their deformation corresponding to the size effects and interaction forces.
- a transform function may exist to link the discontinuous microstress and microdeformation with the continuous macroshear stress and macrodeformation.

2.3 Nanometric cutting model

A comprehensive nanometric cutting model should cover the microstructure of the workpiece and cutting tool, the interaction between the molecules of the cutting tool and workpiece materials. The ideal microstructures of the workpiece and cutting tool can be constructed from their crystal structures, as shown in Fig. 1. The figure shows a typical MD model for nanometric machining, where each atom interacts with its neighbor atoms.

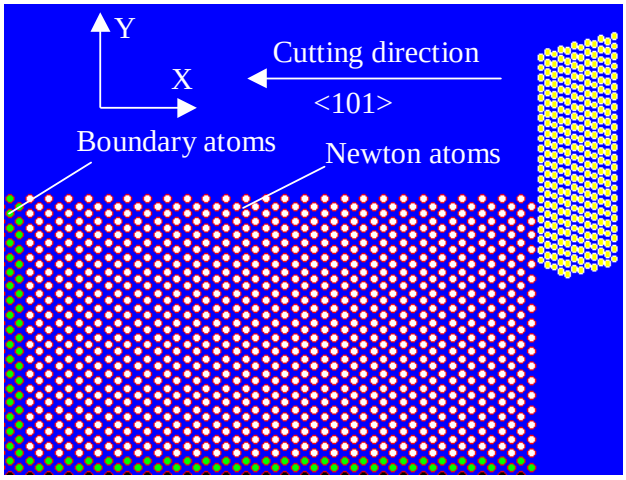

Fig. 1 An MD simulation model for nanometric cutting.

2.4 Cutting energy and cutting forces

The interatomic forces can be computed by the derivation of the potential function of the atoms involved. For example, based on Morse potential function as expressed in equation (1), the interatomic force between atom i and j is:

$$u(r_{ij})=D[\exp(-2a(r_{ij}-r_0)-2\exp(-a(r_{ij}-r_0))] \quad (1)$$

$$F(r_{ij})=-\frac{du(r_{ij})}{dr_{ij}}=2Da[\exp\{-2a(r_{ij}-r_0)\}-\exp\{-a(r_{ij}-r_0)\}] \quad (2)$$

Where D is the cohesion energy, a is the elastic modulus, r_0 is the atomic distance at equilibrium. The force acting on the i-th workpiece atom is obtained by the summation of the interaction with the surrounding atoms as expressed by equation (3)

$$F_{wi}=\sum_{j\neq i}^{N_t}F_{wtij}+\sum_{j\neq i}^{N_w}F_{wwij}=\sum_{j\neq i}^{N_t}-\frac{du(r_{wtij})}{dr_{wtij}}+\sum_{j\neq i}^{N_w}-\frac{du(r_{wwij})}{dr_{wwij}} \quad (3)$$

Where N_t and N_w are the number of cutting tool atoms and workpiece atoms respectively. F_{wtij} and F_{wwij} are the interatomic forces acted on the i-th workpiece material atom from the cutting tool and other workpiece material atoms, respectively. The force on each tool atom is obtained in the same procedure as:

$$F_{ti}=\sum_{j\neq i}^{N_t}F_{ttij}+\sum_{j\neq i}^{N_w}F_{twij}=\sum_{j\neq i}^{N_t}-\frac{du(r_{ttij})}{dr_{ttij}}+\sum_{j\neq i}^{N_w}-\frac{du(r_{twij})}{dr_{twij}} \quad (4)$$

Where F_{twij} and F_{ttij} are the interatomic forces acted on the i-th cutting tool atom from the workpiece material and other cutting tool atoms, respectively.

In general, the cutting forces in nanometric machining are smaller than those in conventional machining because of the smaller depths of cut. Fig. 2 shows the variation of the cutting force in

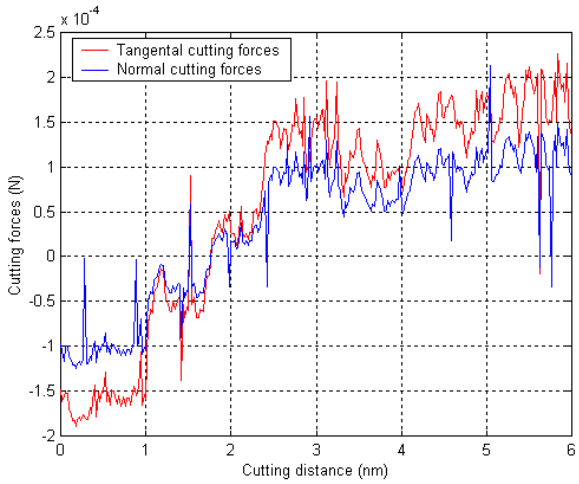

Fig. 2 The variation of the cutting forces during nanometric cutting of single crystal silicon.

a MD simulation of nanometric cutting of single crystal silicon with the cutting edge radius of 30 nm and the depth of cut at 1.76 nm. The simulated mean tangential cutting forces is 55.8 μN. The ratio of mean normal cutting forces to mean tangential cutting forces is 0.66, which is larger than that in conventional cutting. This is because the depth of cut is very small in nanometric cutting, the workpiece is mainly processed by the cutting edge. The compressive interactions will thus become dominant in the deformation of workpiece material, which will therefore result in the increase of friction force at the tool-chip interface and the relative high cutting ratio.

2.5 Molecular movement function

The interatomic forces are the power to stimulate the movement of the atoms within both of workpiece and cutting tool materials. The movement of the atoms is constrained by the Newton's second law as follows:

$$\frac{d^2(r_{wi})}{dt^2} = \frac{F_{wi}(r_{wtij}, r_{wwij})}{m_{wi}} \tag{5}$$

$$\frac{d^2(r_{ti})}{dt^2} = \frac{F_{ti}(r_{twij}, r_{ttij})}{m_{ti}} \tag{6}$$

Where r_{wi} and r_{ti} are the displacement vector of workpiece atoms and cutting tool atoms, respectively.

The loca of the workpiece and cutting tool material atoms can be obtained by resolving equations (5) and (6). If the loca of an individual workpiece atom and cutting tool atom can be obtained, the cutting phenomena can thus be studied at the atomic scale, i.e. at the nanoscale. The mechanisms of the chip removal, the generation of surfaces, tool wear and nanotribological aspects associated with the process can therefore be investigated more precisely and thoroughly.

2.6 Other issues

For a better understanding of the process the following issues in nanometric cutting need to be addressed both qualitatively and quantitatively:

- the radius of cutting edge in relation with the minimum cutting thickness.
- size effects of the tooling and component structures and features, the cutting mechanics will therefore behave very differently at the nanometric scale in particular.
- nanotribological aspects associated with the process, including friction, wear, lubrication, and temperature factors.
- using new analytical and computational tools such as micromechanics and quantum computing, etc.

- quantum effects, statistical time variations of the material properties and their scaling with structure or feature size and dominant surface interactions.

3 MD simulations on nanometric cutting

3.1 A nonlinear MD simulation model

Since the 1980s, Molecular Dynamics (MD) simulation has been employed to study nanometric cutting from the point of view of atomic structure. Belak and Hoover in LLNL and Ikawa and Shimada in Japan are the pioneers of this study [7][8], they have investigated the effect of cutting edge radius and minimum cut thickness in the nanometric cutting process. Inamura in Japan built a model that combined FEM and MDS [9], Rentsch in Germany and Komanduri in USA studied the orientation effects on nanometric cutting processes [10][11]. Komanduri et al. also investigated the effect of tool geometry in nanometric cutting [12]. A sound foundation has been laid, but in their models nonlinear factors and tool wear are not concerned. In nanometric cutting processes, the machined surfaces are very sensitive to the variance of operation conditions, even the micro vibrations between the tool and workpiece surfaces can compromise the productivity and machining accuracy. The machining system should be treated as a nonlinear system since there are many nonlinear sources in association with the processing, machine tool, tooling and workpiece materials [15]. They include:

- loss-of-contact;
- mode coupling (cutting force coupling);
- tool wear;
- structural and contact stiffness and damping in machine tool structure;
- workpiece strain hardening and softening, strain-rate dependence, thermal softening;

- regenerative chatter;
- the irregular elastic recovery of the machined surfaces;
- friction and lubrication, etc.

Because the cutting forces are obtained from the atomic interaction forces, some nonlinear sources such as the mode coupling and regenerative chatter, irregular elastic recovery of the

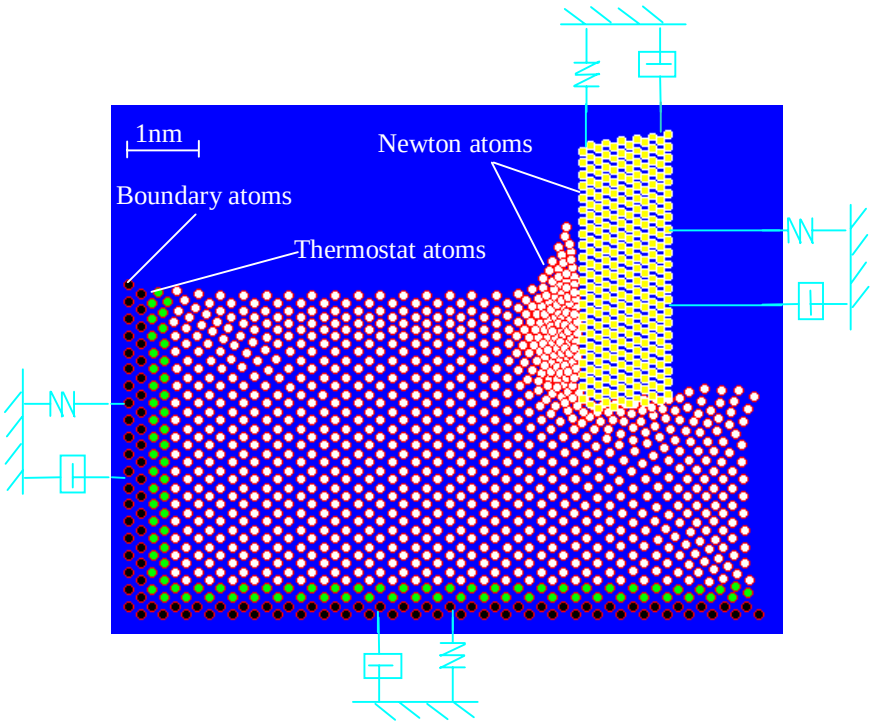

Fig. 3 A nonlinear MD simulation model for nanometric cutting.

machined surfaces, and the friction and lubrication result in the variance of cutting forces. The MD modelling and simulation should cover these sources. With regarding to the structural and contact stiffness and damping in the machine tool/tooling/workpiece structure, the nonlinear MD simulation model has been developed as illustrated in Fig. 3. In this model the tool wear is still neglected in order to investigate the other isolated nonlinear effects on the machining. As shown in Fig. 3, the material is divided into three different zones, called the Newton atoms zone,

thermostat atoms zone and the boundary atoms zone. The boundary atoms are fixed in position but with an average displacement of new atoms calculated with equation (7). The lattice vibration is thus neglected and the boundary effects are reduced and the proper symmetry of the lattice maintained. Thermostat atoms are scaled to control the processing temperature. The atoms in the Newton atoms zone and the cutting tool are regarded as Newton atoms which behave according to the Newton's second law. The action between the diamond tool and workpiece material is calculated by the Morse potential function. The motion of the Newton atoms and thermostat atoms in workpiece are determined by equation (7):

$$m_i \ddot{r}_i + \frac{h_c}{\omega}\dot{r}_i + \lambda_s(r_i + \beta_{c1}r^2 + \beta_{c2}r^3) + \lambda_a r_i = F(r_i) \tag{7}$$

where m_i is the mass of the atom calculated, h_c is hysteric damping constant and ω is the chatter frequency. λ_s and λ_a are the slope of the stiffness function at origin and the inter-atomic stiffness coefficient, respectively. β_{c1} and β_{c2} are nonlinear constant coefficients of stiffness function. The revised Verlet algorithm is deduced to make the numerical error minimum. The displacement r_i^{n+1} and velocity v_i^n are given by equations (8) and (9):

$$r_i^{n+1} = r_i^n(1-\frac{h^2}{2m_i}\lambda_a - \frac{h^2}{2m}\lambda_s) + hv_i^n(1-\frac{h\cdot h_c}{2m\omega}) - \frac{h^2}{2m_i}F_i^n - \frac{h^2}{2m_i}\lambda_s[\beta_{c1}(r_i^n)^2 + (\beta_{c2}(r^n{}_i)^3] \tag{8}$$

$$\begin{aligned} v_i^{n+1} = {} & \frac{\omega + h_c}{\omega - h_c}v_i^n + \frac{\omega h}{2m_i(h_c+\omega)}[(F_i^n + F_i^{n+1}) - (\lambda_s + \lambda_a)(r_i^n + r_i^{n+1}) - \lambda_s\beta_{c1}[(r_i^n)^2 + (r_i^{n+1})^2] \\ & - \lambda_s\beta_{c2}[(r_i^n)^3 + (r_i^{n+1})^3] \end{aligned} \tag{9}$$

Where h is the integration time. Typically the initial positions of the material atoms and tool atoms are the sites on a face-centered cubic (f. c. c.) lattice and diamond lattice, respectively. The initial velocities are assigned from a Maxwell distribution at room temperature (20 °C). Through the iterative calculations with equations (8) and (9), the displacement of atom i at time $n+1$ and its velocity at time $n+1$ can be determined. The deformation or fracture process of the nanometric

cutting can then be studied through the modelling and computation mentioned above at the atomic level.

3.2 The generation of machined surfaces

The nanometric orthogonal cutting on the (001) plane of a mono-crystalline aluminum using a diamond tool with the cutting edge radius of 0.35 nm is simulated, where the uncut chip thickness and the cutting speed is set at 1.4 nm and 20 m/s, respectively. The cutting speed is higher than that in reality in order to reduce the computing time. The cutting direction is taken at $<0\bar{1}0>$. The time step is 34 fs. The initial temperature is 20 °C. The rake angle of the tool is 0° and the

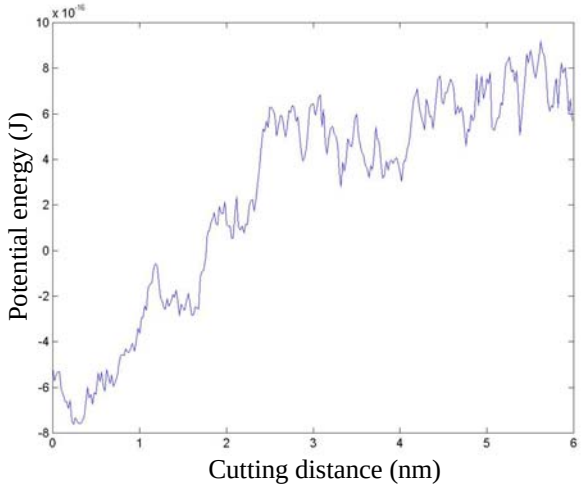

Fig. 4 The variance of potential energy during the nanometric cutting process.

clearance angle is 10°. The workpiece material presented in the simulation presumes containing 3,516 Al atoms and the cutting tool containing 1,931 diamond atoms as limited by the computing power. The chip removal and the generation of machined surfaces are the result of the cutting process.

The variance of the potential energy during the machining process is shown in Fig.4. It shows that the potential energy is negative before the approaching of the cutting tool and it then

becomes positive at tool engagement. There is a drastic variance of the energy in the cutting process probably owing to the nonlinear sources.

Fig. 5 shows a snapshot of the nanometric cutting process obtained by MD simulations. It can be seen that the chip is removed with the unit of an atomic cluster. Based on the results shown in Fig. 4 and Fig. 5, the generation of nanometric cut surfaces can be explained as below. Due to the plowing of the cutting edge, the attractive force between the workpiece atoms and the diamond

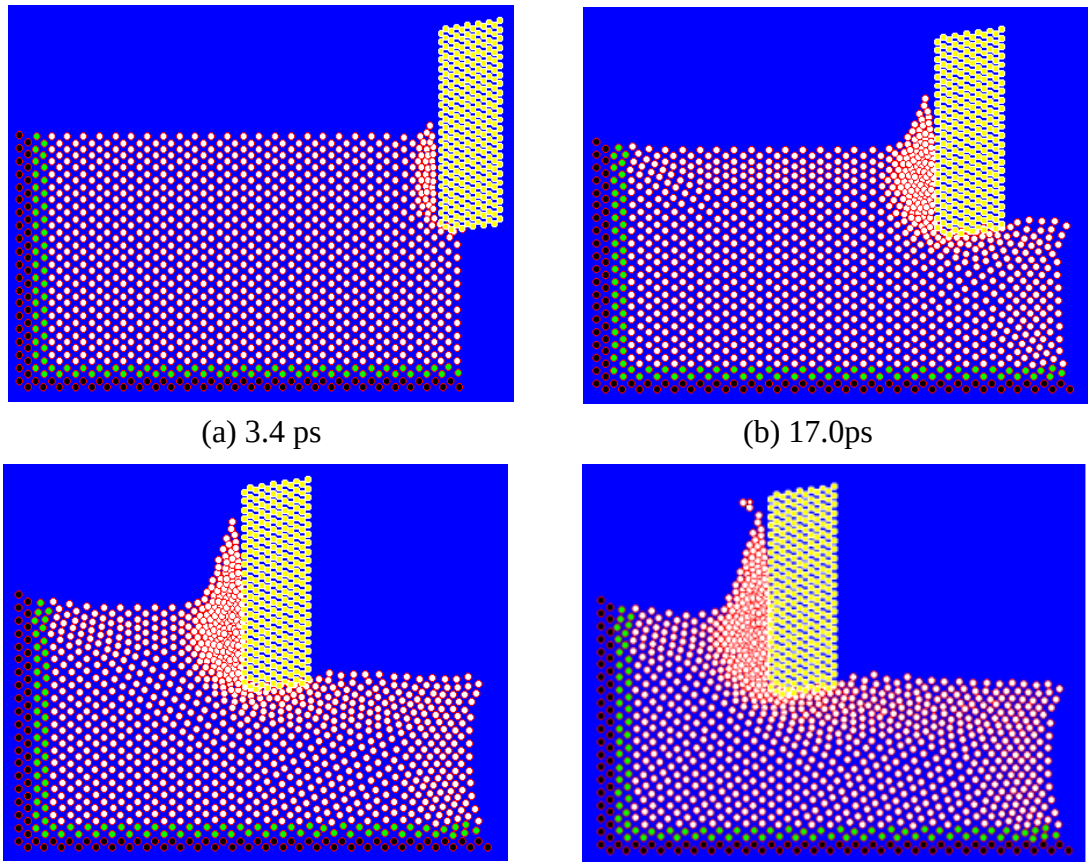

(a) 3.4 ps (b) 17.0ps

(c) 30.6 ps (d) 37.2 ps

Fig.5 MD simulations of the nanometric machining process.

tool atoms becomes repulsive. Because the cohesion energy of diamond atoms is much bigger than that of Al atoms, the lattice of the workpiece is compressed. When the strain energy stored

in the compressed lattice exceeds a specific level, the atoms begin to rearrange so as to release the strain energy. When the energy is not sufficient to perform the rearrangement, some micro-dislocations are generated. Repulsive forces between compressed atoms in the upper layer and the atoms in the lower layer are increasing, so the upper atoms move along the cutting edge, and at the same time the repulsive forces from the tool atoms cause the resistance for the upward chip flow to press the atoms under the cutting line. With the moving of the cutting edge, some dislocations move upward and disappear from the free surface when they approach the surface. This phenomenon corresponds to the process of the chip formation. As a result of the successive generation and disappearance of dislocations, the chip seems to be removed steadily. After the passing of the tool, the pressure at the flank face is released. The layers of atoms move upwards and result in elastic recovery, so the machined surface is generated. The conclusion can therefore be drawn that the chip removal and machined surface generation are in nature the dislocation slip movement of workpiece materials.

3.3 Cutting tool wear

The nanometric cutting of single crystal aluminum is taken as the case study on tool wear. Fig.6 shows the 3D MD simulation model for orthogonal cutting at the (001) plane of monocrystalline aluminum by the diamond cutting tool. The model contains about 90,000 atoms of workpiece and tool materials. The thermostat atoms control the process temperature. In order to reduce the boundary effects, the hard boundary condition is adopted. The cutting edge radius of the diamond tool is 1.3 nm, the uncut chip thickness is set as 1.5 nm. The cutting speed of 100 m/s is employed to reduce the computation time. Although this cutting speed is unrealistic, it was proved that there was little difference between the surface quality obtained under the cutting speed between at 20m/s and 200m/s as presented by Shimada et al [16]. For the Al-Al

interactions in the workpiece and C-C interactions in the diamond tool, the modified embedded-

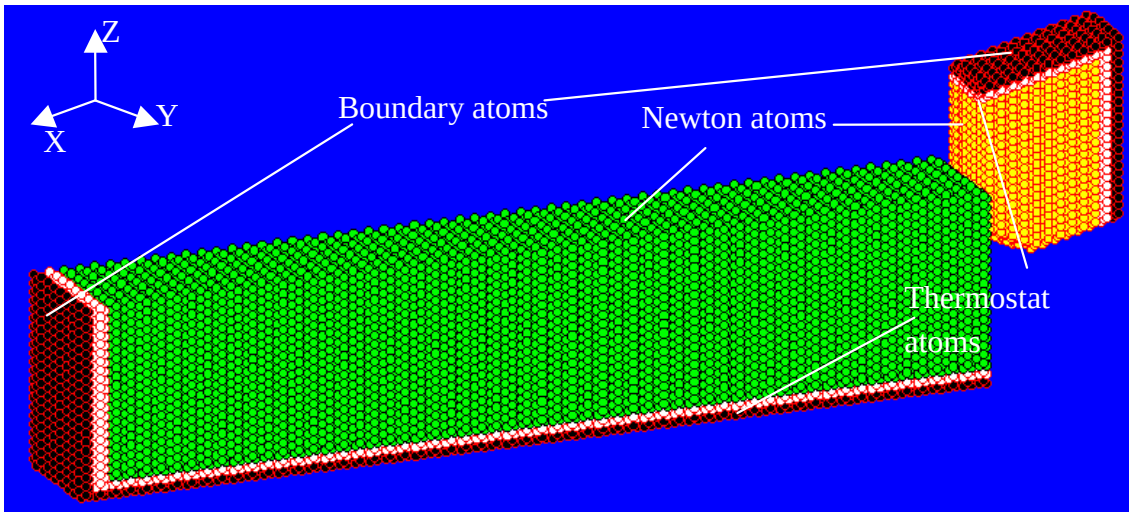

Fig.6 The 3D MD model for nanometric cutting.

atom potential is employed [17]. In this model the thermal effects of cutting heat on the nanometric cutting is included by the algorithm of adjusting the sublimation energy parameter of aluminum atom and carbon atom according to the variance of temperature. It is based on the calculation of the equilibrium temperature of the cutting system through the theorem of equipartition of energy, and the enthalpy of sublimation of aluminum atom and carbon atom through Kirchhoff's law. In this canonical ensemble due to the constant pressure, the enthalpy of sublimation of the aluminum atom and the carbon atom equals to their sublimation energy. According to the relationship between the sublimation energy and the temperature, we can rectify the sublimation energy in MEAM potential. Because the difference of potential will be the interatomic forces, thus the effect of cutting heat is added in the cutting system. The detail algorithm has been deducted in reference [18] by the authors.

In order to clearly observe the tool wear, the snapshots of the work and tool atoms at the section of (200) plane are showed in Fig. 7 at the different times of 20.4ps (a) and 120ps (b) from the beginning. At 20.4 ps, the crystal state of the work material under the cutting edge and the

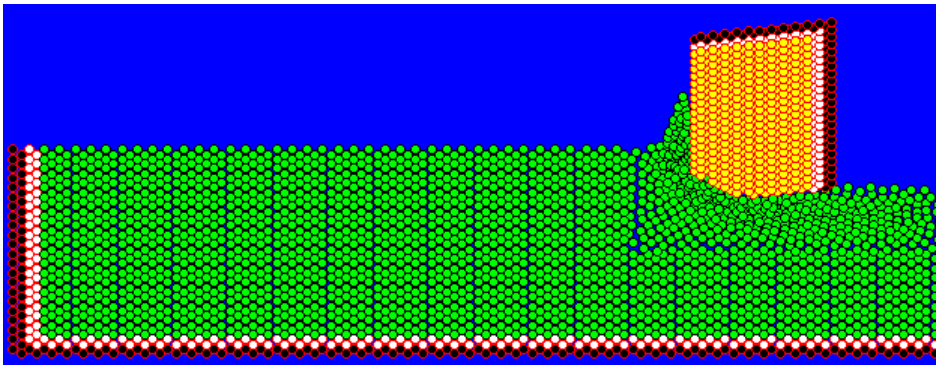

(a) 20.4 ps

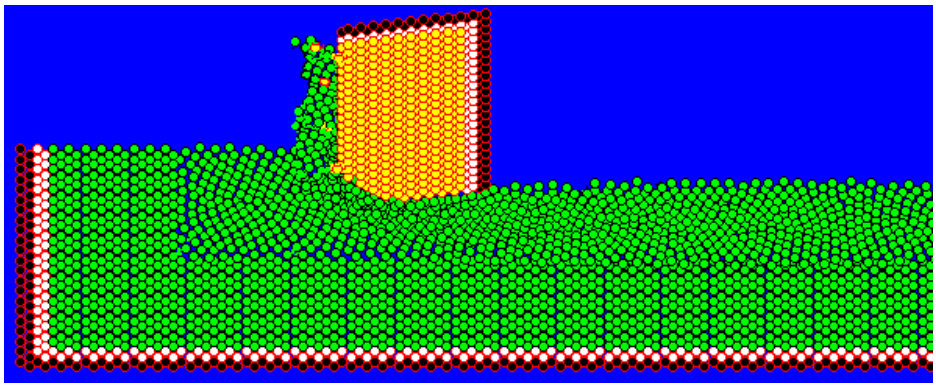

(b) 120 ps

Fig. 7.4 MD simulation snapshots at different times steps.

rake face begins to be disturbed. At 120 ps, there are distinct diffusions between the work and tool atoms. A few tool atoms at the tip of the tool are separated, and then move with the chip and only several of them adhere to the cutting edge and diffuse with work atoms on the rake face. But the shape of the cutting edge has already been changed, which indicates the cutting edge of the tool begins to wear. The phenomenon is the result of a rapid rise of the temperature in cutting zone. The sublimation energy of C remarkably decreases with the increase of cutting temperature. In contrast, the variance of the sublimation energy of Al is very small. The decrease of the carbon

sublimation energy will result in the weakening of the C-C covalent bond, and cause the decrease of the cohesion energy of diamond atoms. With the increase of the kinetic energy of work atoms, some work atoms diffuse with the tool atoms. The diffusion of the work atoms can weaken the bonding of tool atoms. Furthermore, the weakened bonding of diamond atoms may promote the diffusion of the work atoms in turn. According to the stress calculation in reference [121], the maximum stress in workpiece is founded right at the interface with the tip of the tool. This suggests that the tip of the tool is apt to wear, which has been proved by the simulation results as illustrated in Fig.7.4 (b).

4 The test-bed for nanometric cutting

4.1 Nanometric cutting trials with atomic force microscope (AFM)

There is no doubt that the knowledge on the physics of nanometric cutting can be acquired directly by nanometric cutting trials on an ultra-precision machining tool. However, the development of atomic force microscope (AFM) techniques provided alternative way to fulfill it. The sharp diamond tip of AFM has been utilized to emulate a single-point diamond cutting tool in cutting the workpiece surface by other researchers [19][20] to study the nanometric cutting mechanism, albeit the tip is normally used to acquire surface topography by scanning the surface. Although the torque stiffness of the cantilever of AFM is lower than that of a conventional tool-holding arrangement and the normal load of the AFM is smaller than conventional work-tool contact load, the material removal process in nanometric cutting using AFM is very similar to that using a diamond cutting tool [20]. Moreover, the material removal volume of nanometric cutting with AFM is just consistent with the scale of current MD simulation. Therefore, the nanometric cutting trials were carried out on a single crystal silicon plate by the diamond tip of

an AFM (Nanoscope IIIa Dimension 3100, Digital Instruments) in scratching mode. The diamond tip cutting edge radius is 30 nm, and the torque stiffness of the cantilever is 2.9×10^{-5} N/V (as provided by the manufacturer). In the trials, the normal load keeps 40 μN during the indentation and scratching process, and the frequency of the scanning is set at 1 Hz. The scratching process is repeated after the diamond tip indenting the surface to some extent until the

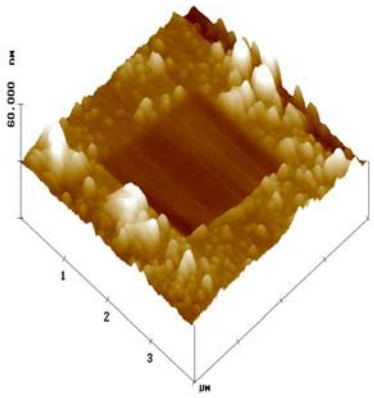

Fig. 8 Machined surface topography.

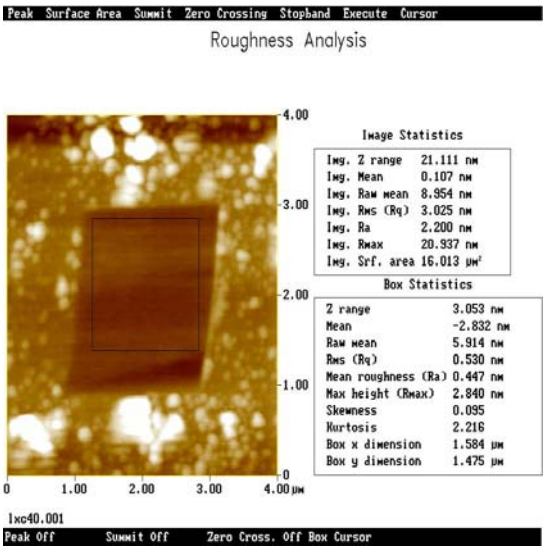

Fig. 9 Surface roughness analysis.

generation of a machined surface area of 2 μm by 2 μm. The texture image of the machined surface and its surface finish analysis diagram are shown in Fig. 8 and Fig. 9 respectively. The surface mean roughness Ra is measured as 0.447 nm. The results show that nanometric cutting with a diamond cutting tool can be achieved predictably and productively. Furthermore, based on the signal of torque voltage and the stiffness of cantilever, the cutting force can be calculated as 67.4 μN. The force value is quite consistent with that forecasted by the nanometric cutting MD simulation as described in section 2.4 ($\frac{67.4-55.8}{67.4}\times100\% = 17.2\%$ difference).

4.2 Bench type ultraprecision machine tools for nanometric cutting

Fig. 10 shows the conceptual design of a bench type ultraprecision machine tools for nanometric cutting proposes. The machine aims to be an ultraprecision machining facility for manufacturing 3D MEMS devices.

The machine has the following features:

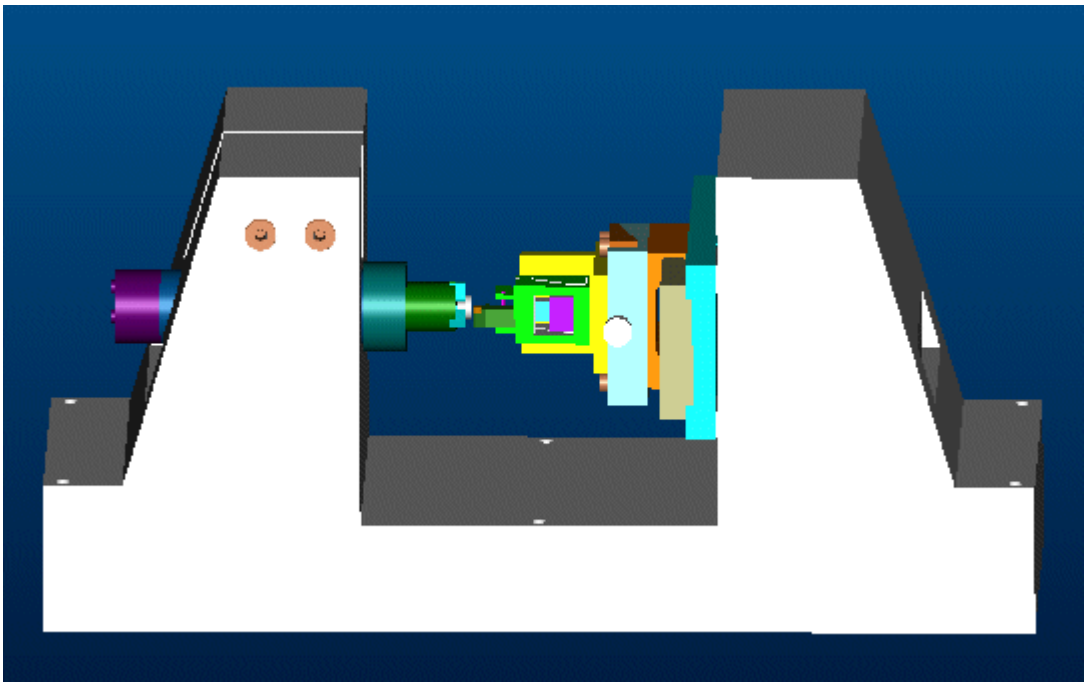

Fig. 10 Layout of a bench type ultraprecision machining tools for nanometric cutting.

- Bench type for the benefits of low cost, industrial feasibility and ease of localized environmental control.
- Modular structure to enable a flexible implementation of developed technology and products and to help with customization.
- Use of a linear-motor and a piezoelectric actuator for motion control combined with a smart manually adjustable unit.

The machine is currently at the stage of assembly and testing. The authors would like to report the detail of the machine development in the near future.

5 Concluding remarks

In this paper the mechanics of nanometric cutting is investigated with the aid of MD modelling and simulations and the cutting trials on an AFM. The physics of nanometric cutting is characterised in comparison with the conventional machining process. The features and characteristics of nanometric cutting are further clarified by MD simulations and the cutting trials. The authors believe a combination of theoretical (analytical and computational), simulation and experimental methodologies is essential to address the underlying necessities for the predictability, producibility and productivity in manufacturing at the nanometric scale.

6 Acknowledgments

The authors would like to thank Loadpoint Ltd for their support for the part of this research.

References

[1] CORBETT, J., MCKEOWN, P. A., PEGGS, G. N., and WHATMORE, R., 2001, Nanotechnology: international developments and emerging products. *Annals of the CIRP*, 49 pp. 1-23.

[2] Natural Science Foundation in the USA, 2001, Nanomanufacturing program information (http://www.eng.nsf.gov/dmii/DMIIDivdescription.doc).

[3] CHENG, K., LUO, X., and WEBB, D., 2001, A novel systematic approach to modelling precision-machined surfaces based on mathematical transforms. Proceedings of Fifth

International Conference on Laser Metrology, Machine Tool, CMM and Robot Performance, Birmingham, UK, pp. 259-268.

[4] SHAW, M. C., 1984, *Metal Cutting Principles* (Oxford: Oxford University Press).

[5] TRENT, E. M., 1984, *Metal Cutting* (London: Butterworth).

[6] OXLEY, P. L. B., 1989, *The Mechanics of Machining: An Analytical Approach to Assessing Machinability* (Chichester: Ellis Horwood Limited).

[7] BELAK, J., BOERCKER, D. B., and STOWERS, I. F., 1993, Simulation of nanomerter-scale deformation of metallic and ceramic surface. *MRS Bulletin,* 18, pp. 55-60.

[8] IKAWA, N., DONALDSON, R. R., KOMANDURI, R., et al, 1991, Ultraprecision metal cutting-the past, the present, and the future. *Annals of the CIRP*, 40 pp. 587-594.

[9] INAMURA, T., SUZUKI, H., and TAKEZAWA, N., 1990, Cutting experiment in a computer using atomic models of a copper crystal and a diamond tool. *International Journal of Japanese Society of Precision Engineering,* 56, pp. 1480-1486.

[10] RENTSCH, R., 2001, Influence of crystal orientation on the nanometric cutting process. Proceedings of 1st International euspen Conference, Bremen, Germany, pp. 259-268.

[11] KOMADURI, R., Chandrasekaran, N., Raff, L. M., 1999, Orientation effects in nanometric cutting of single crystal materials: an MD simulation approach. *Annals of the CIRP*, 48, pp. 67-72.

[12] KOMADURI, R., CHANDRASEKARAN, N., RAFF, L. M., 1998, Effect of tool geometry in nanometric cutting: a molecular dynamics simulation approach, *Wear*, 219, pp. 84-97.

[13] SHIMADA, S., TANAKA, H., and IKAWA, N., 1999, Atomic mechanism of surface generation in micromachining of monocrystalline silicon. Proceeding of the 1st international euspen conference, Bremen, Germany, pp. 230-233.

[14] LUCCA, D. A., SEO, Y. W, and RHORER, R. L, 1994, Aspects of surface generation in orthogonal ultraprecision machining. Annals of the CIRP, 43, pp. 43-46.

[15] WIERCIGROCH, M., and KRIVTSOV, A. M, 2001, Frictional chatter in orthogonal metal cutting. *Philosophical Transactions of the Royal Society,* A359, pp. 695-713.

[16] SHIMADA, S., IKAWA, N., TANAKA, H., et al., 1994, Structure of micromachined surface simulation by molecular dynamics analysis. *Annals of the CIRP*, 43, pp. 51-54.

[17] BASKES, M. I., 1992, Modified embedded-atom potentials for cubic materials and impurities. *Physical Review,* B 46, pp. 2727-2741.

[18] LUO, X., LIANG, Y., DONG, S., and ZHAO, Q, 2000, Atomic analysis of nanometric cutting process by a new MD simulation approach including thermal cutting effects. Proceedings of 1st euspen International Conference on Fabrication and Metrology in Nanotechnology, Copenhagen, Denmark, pp. 161-168.

[19] ZHAO, X, BHUSHAN, B., 1998, Material removal mechanisms of single-crystal silicon on nanoscale and at ultralow loads. *Wear*, 223, pp. 66-78.

[20] ZHAO, Q., and DONG, S., 2001, Investigation of single asperity microcutting using an Atomic Force Microscope. Proceedings of the euspen 2nd International Conference, Turin, Italy, pp. 632-635.